Optimization of a Diver Propulsion Vehicle Hydrodynamics Parameter and its' Shape Improvement by CFD Method for Improving Underwater Speed Record

M. R. Sadeghizadeh[1], B. Saranjam[1] and R. Kamali[2]

[1]*Department of Hydro-Aerodynamic Research Center of MUT University, I. R. Iran*
[2]*School of Mechanic Engineering , Shiraz University, I.R. Iran*

†*Corresponding Author Email: mr_sadeghizadeh@yahoo.com*

ABSTRACT

The hydrodynamic shape of high speed diver propulsion vehicle (DPV) is very important to its performance. One of the basic optimization steps is minimizing DPV drag force to reduce power required. In the present paper, the research has been started by optimization process with a basic design and it would be gradually improved to achieve favorable hydrodynamic characteristics according to diver size and his required volume. The main target is minimizing lift and drag force as objective function. Moreover, this optimization scenario is applicable and it has been followed on the real DPV prototype. The prototype has been constructed and tested in towing tank for results validation. The 3D geometry of a real diver has been created by image processing and software modeling. According to this model the first basic geometry had been designed and then it has been exported to CFD code for steady-state computational analysis. The *SST-Kω* turbulence model has been selected in the solution to compute hydrodynamic forces. So the position of propulsion system and the shape of vehicle have been improved by repetition process. Output results show that the drag values will be significantly reduced with shape improvement about 51 percent in design speed.

NOMENCLATURE

D_t	total drag force	u_j	Y- velocity component
k	turbulent kinetic energy per unit mass	$\overline{u}_j$	instantaneous term of Y- velocity component
L	vehicle length		
P	pressure	u'_j	fluctuation term of Y- velocity component
P_p	propulsion power		
Re	Reynolds number	$\vec{u}$	velocity vector
t_{ij}	stress tensor		
U	free stream or DPV velocity	η_p	propulsion efficiency
u_i	X- velocity component	μ	dynamic viscosity
u'_i	fluctuation term of X- velocity component	υ	kinematic viscosity
		ω	specific dissipation rate
$\overline{u}_i$	Instantaneous term of X- velocity component	ρ	water density
		τ_{ij}^t	reynolds stress

1. INTRODUCTION

A diver propulsion vehicle, also known as underwater scooter that it has been used by diver is an item of diving equipment to increase range and speed and ease underwater diving. Generally, the range is restricted by the amount of breathing air that can be carried by each diver and the rate at which his breathing is consumed air under exertion and the time limits imposed by the dive tables to avoid

decompression sickness. Though, a DPV usually consists of a propeller which is driven by DC electric motor. The design of DPVs should be satisfied all diver safety standards to ensure propeller disservice and its harmless to diver or other diving equipment, Frederic (2010).

Constructing a prototype of an electrically actuated thruster as a direct drive propulsion system based on a 3-phase permanent magnet brushless machine for an autonomous underwater vehicle was presented by Ishak, (2010). It was one of the works that focused on propulsion unit. A diver could be carried by a DPV as a scooters or propulsion unit attached to legs, arms or air tank.

Researchers choose a suitable DPV hydrodynamic shape in order to reduce unwanted wake and minimize drag force to redound in lower power consumption. The design of underwater vehicles has been introduced especially in the mid1980s by many researches like Smallwood work (1999) and since then they have been developed with the fast rate. These vehicles came into a new era as they were able to operate faster and going to more depths below commercial diver limits.

Griffiths and Edwards (2003) have been done a master research work in designing and operating DPV as a next generation vehicles. The design of such submersible vehicle should be passed many safety standards and real tests, Allmendinder (1990). On the other hand, in designing of high performance DPVs good CFD methods should be used to evaluate their hydrodynamic force and moment.

Previously, the ability of applying CFD to solving underwater motion had been shown by Bixler and Schloder (1996), when they used a 2D-CFD analysis to evaluate the effects of accelerating of a flat circular plate through water. They improved latest work with other research in 2002 and calculated the coefficients of hydrodynamic force in steady-state 3D-CFD analysis and they revealed the well compatibility of their results with experiments, (2002). You should be perpended that experimental investigation of underwater motion is very difficult and there are more complexity that arisen from transient nature of the flow. On the other hand computational fluid dynamic for modeling of underwater vehicle motion implies many details of the flow field around it. This allows to scrutinizing the flow behavior and understanding of the fluid dynamics. Also, there are many turbulence in the flow that they are participated by free surface time dependent deformation and existence of air-water mixture that related to the flow structures that should be studied truly. Cohen *et al.* (2009) presented a new method named mesh-free smoothed particle hydrodynamic (SPH) that was ideally capable to overcome many of these difficulties.

In other research Ramos *et al.* (2012) was investigated the effect of body positions on drag during the streamlined glide in swimming by CFD method. Anyway, the application of CFD for evaluating of underwater motion is undeniable.

One of the most important branches in this field is optimizing of underwater vehicles.

Tahara *et al.* (2006) presented CFD-based multi-objective optimization method for ship design. Their method had been based on three main steps: geometric model generation, CFD calculation and module of optimization.

The author in other research in 2016 presented the experimental and numerical investigation of high speed swimmer motion in different depths from free surface. In this work the swimmer motion was simulated in high speed based on reliable CFD method and the numerical outputs have been validated by towing tank experiment (2016). Increasing diver's underwater speed can cause many problems for diver like air mask movement and respiration tribulation, encountering obstacles through reduced vision, unwanted cyclic going deep and back that follow narcosis. A suitable diver propulsion vehicle should be designed for overcoming to these problems. Of course, it is important to provide diver safety in each condition like high speed motion.

Hence, to increase diver speed a water shield must be designed for him to ensure implicit levels of safety. Anyway, the design of auxiliary equipment such as this vehicle that enables the diver to attain higher speed is a new challenge in the underwater high speed motion field. Whereas the actual test of new equipment of this type is very expensive and there are many difficulties involved in conducting such work experimentally, the use of CFD method developed day after day. Now, the CFD method is recognized as an acceptable approach to calculate the best solution of problem like this.

In addition to designing a vehicle with low drag and high power characteristics, a good CFD method has other advantage by showing detailed characteristics of fluid flow around the vehicle. But by CFD alone you do not be able to design the best one and you should be arranged a scenario that will be applied many design experience and optimization process together.

Whereas the DPVs have multipurpose application like military there are a little literatures about high speed one. The present paper was an attempt to showing the method of modification and optimization of a practical diver propulsion vehicle by combining CFD with the best turbulence model and design experiences in order to minimize unfavorable hydrodynamic forces to receive high performance underwater high speed motion as a new point of view. The main aim of this work is to specify how DPV speed could be increased with optimized configuration without any risk to diver according to CFD technique and then by towing tank experimental outputs.

Moreover the best minimum depth of motion and his power required has been determined. This work introduced asseveration about maximum DPV speed test worldwide that is twice the other work heretofore as a special novelty.

2. GOVERNING EQUATION AND TURBULENCE MODEL

The Reynolds number is the primary non-dimensional parameter in low speed flows concern under consideration. This parameter represents the ratio of inertial to viscous forces in the flow and defined as:

$$Re = \rho\, U\, L\, /\, \mu = U\, L\, /\, \upsilon \tag{1}$$

Where U is the speed that simulated free-stream velocity and υ is the fluid kinematic viscosity. The characteristic length (L) can be selected as the length of the vehicle. On the other hand the minimum length of the vehicle is obtained from the length of the real diver with open hand as in optimization process this value is the one of the basic limitation that must be considered in the overall calculation.

In many cases, the drag coefficient is reasonably independent of Reynolds number upon a critical value is exceeded. Though in complex shape with different parts they may be exposed to different velocity condition there is less chance of this independence as different parts of the vehicle subjected to different Reynolds numbers. As the vehicle may be exposed to a range of flow speeds, it might be necessary to simulate a range of Reynolds numbers to get a more complete prospect of the loads that will be encountered in actual motion.

The minimum Reynolds number according to minimum length of the vehicle in this study is about 15.95 e6 that is assumed fully turbulent condition. The governing equations explained the conservation laws of flow in mathematical forms. These laws are as follow:

Continuity eq.:

$$\vec{\nabla} \cdot \vec{u} = 0 \tag{2}$$

Momentum eq.:

$$\frac{\partial}{\partial x_j}\left(\rho u_i u_j\right) = -\frac{\partial P}{\partial x_i} + \frac{\partial t_{ij}}{\partial x_i} + \frac{\partial \tau_{ij}^t}{\partial x_i} \tag{3}$$

In this equation the stress tensor t_{ij} and Reynolds stress term τ_{ij}^t are as follow:

$$t_{ij} = \mu\left(\frac{\partial u_i}{\partial x_j} + \frac{\partial u_j}{\partial x_i}\right), \quad \tau_{ij}^t = \overline{-\rho u_i' u_j'} \tag{4}$$

Since in turbulent flow the actual velocity of each particle is the sum of instantaneous and fluctuation component. The last term $\overline{\rho u_i' u_j'}$ that is named Reynolds stress should be obtained with favorable turbulent models. There are different turbulent models in computational fluid dynamic which should be selected according to nature of flow, required accuracy, calculating facilities and computational time.

This is an active field as the researchers have been published many papers to demonstrate which one is more efficient relative to other models with the same conditions.

For example, Zaidi *et al.* (2010) was presented a paper to specify which model of turbulence is the most adapted in order to predict drag forces. They showed that *SST k-ω* model is an accurate one. According to this model the **k** and **ω** are:

$$\frac{\partial}{\partial t}(\rho \boldsymbol{k}) + \frac{\partial}{\partial x_i}(\rho \boldsymbol{k} u_i) =$$

$$\frac{\partial}{\partial x_j}\left(\Gamma_k\, \frac{\partial \boldsymbol{k}}{\partial x_j}\right) + \boldsymbol{G}_k - \boldsymbol{Y}_k + \boldsymbol{S}_k \tag{5}$$

$$\frac{\partial}{\partial t}(\rho \boldsymbol{\omega}) + \frac{\partial}{\partial x_i}(\rho \boldsymbol{\omega} u_i) =$$

$$\frac{\partial}{\partial x_j}\left(\Gamma_\omega\, \frac{\partial \boldsymbol{\omega}}{\partial x_j}\right) + \boldsymbol{G}_\omega - \boldsymbol{Y}_\omega + \boldsymbol{S}_\omega \tag{6}$$

The parameter "$\boldsymbol{\omega}$" is the rate of energy dissipation per unit volume per time (or specific dissipation rate) and "$\boldsymbol{k}$" is the turbulent kinetic energy per unit mass.

Hence, with obtaining the drag forces by this method for a diver propulsion vehicle, the propulsion power related to require speed could be calculated:

$$P_p = D_t \cdot U \tag{7}$$

On the other hand, if it was assumed that electrical power is going to be used for propelling him other parameters enter the problem, like propulsion efficiency (that is composed of propeller and motor efficiency) and weight geometry of such system. Thus the installed power P_i is defined for this condition as Eq. (8):

$$P_i = \frac{P_p}{\eta_p} \qquad (\eta_p = \text{propulsion efficiency}) \tag{8}$$

The hydrodynamic forces in underwater motion highly have been related to moving body shape and geometry. For example, there are strong separation at all sharp corners of rectangular cylinder that it will be caused very high drag force. While by rounding these sharp edges the drag will be reduced about 45 percent. Nevertheless, the important part of the cylinder is the half rear end or cylinder trailing edge region which by streamlining this part to a quoin shape the pressure drag will be reduced 85 percent more than before for the given diameter. Therefore the aft body shape is very important to reduce hydrodynamic drag force and the fore and aft shape should be optimized for high-performance vehicles. As mentioned above, the relative contribution of drag depends upon the body's shape and configuration and the importance of shape optimization is inevitable.

Hence the authors have been arranged a methodology for DPV optimization by combining model reconfiguration with CFD calculation loop to create a progressive optimization solution. It has been based on four main steps; Geometry implementation, Grid manipulation, CFD calculation and constraints evaluation, (Fig.1).

This work has been started with a primary shape with given length and frontal area and then by iterative process this shape has been improved in model reconfiguration and CFD calculation loop. In the

CFD calculation the *SST k-ω* model of turbulence has been considered for numerical simulation and whereas the main target is reaching to speed up to 6 m/s the motion occurred in deep water and the effect of free surface has been neglected.
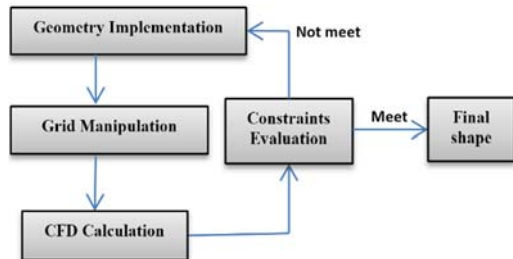

Fig. 1. Basic elements of the CFD-based method of optimization.

3. DPV MODELING AND NUMERICAL SIMULATIONS

While an overall optimization problem has been considered the main goal is minimizing the cost function of hydrodynamic drag according to required speed. But it should be recognized two other parameters, lift force and pitching moment consequently. So it should be defined the important factors that affected these parameters. This has been done in model implementation module by the basic concept that when the flow accelerated over high convex shape its pressure will be dropped in this region and vice versa.

The first step for this optimization process is generating of a suitable diver model. We selected a real diver and modeled him with 3D image processing. Then, the DPV model has been designed with the best ergonomic shape as the diver could be set on it as a preliminary geometric law for each model generation in geometry implementation module. There are a lot of experiences in designing underwater body configuration derived from shark or dolphin nose shape which they should be adjusted to the DPV nose with preserving his minimum required volume in the vehicle. The first produced geometry has been shown in (Fig. 2).
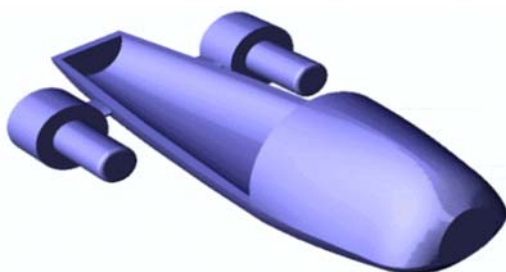

Fig. 2. The first design of DPV model.

The preliminary dimensions of the first DPV had been selected as 2m×0.7m×0.7m (length ×width× height). It is based on real prototype that had been presented for production. That was an improvement

vehicle similar to K-10 TNT Marine Enterprises diver training propulsion vehicle. The following restrictions have been considered in generating each computational model. In fact these restrictions have been imposed in *Geometry Implementation* module as fixed design parameters:

a) $A_{frontal} = A_{ref.}$ (9)

(Fixing one of the main parameter that will be affected the drag force)

b) $L_{min} \geq k$ (10)

(Length limitation for introduced volume constraint of diver by coupling to frontal area)

The limitation of inner vehicle volume will be leaded to a minimum frontal area ($A_{ref.}$) for diver accommodating on it with thruster unit. This value is the minimum area required to one normal person occupation in prone position ahead to flow stream in addition to thruster unit. Meanwhile the minimum length of vehicle is selected as the minimum required length k from vehicle nose to diver waistline.

A calculating domain with suitable dimensions has been generated after implementing the first model. The length and width of geometric domain have been selected as three tenfold vehicle lengths for domain length and about tenfold the width of vehicle for domain width, (Fig.3).
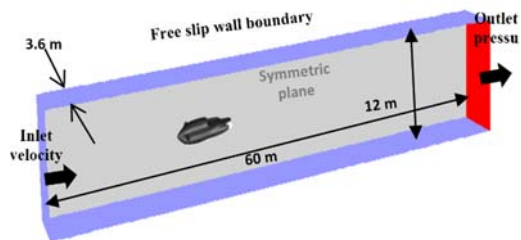

Fig. 3. The domain geometry built around the model.

The satisfaction of domain dimensions is evaluated as the velocity of fluid stream remains unchanged on domain boundary walls compared with inlet velocity. At first the domain is separated to two parts and joined together one for vehicle body and the other for thrust unit but it will be entered more complexity and more calculating time with a little gain. One part is fixed and the other part that related to propeller size is rotated with propeller speed (about 800 revolutions per minute). But the rotated part has been deleted in further steps. Half of the model has been considered in solution because of the problem symmetry situation. The un-structure pyramid elements have been used for mesh generation and furthermore 40 boundary layer elements have been set on it for more accuracy, (Fig. 4).

The mesh independency analysis was accomplished by 11.3e6, 13.03e6, 15e6 and 16.5e6 cells (table 1). The results showed that to obtaining accurate output with saving computational time, the third one with respect to last one is preferable and had no significant difference, so this grid has been selected and used for other optimized geometry (grid manipulation step).

The parameters that guarantee CFD accuracy should be checked in numerical calculation. The first parameter is Y^+ which must be less than 10 for *SST-Kω* turbulence model. The law of the wall that has been known as Y^+ is a dimensionless distance from each wall surface and it should be appropriated value to get the acceptable solution. The Y^+ distribution has been shown in Fig.5 for final shape in speed of 6 m/s.
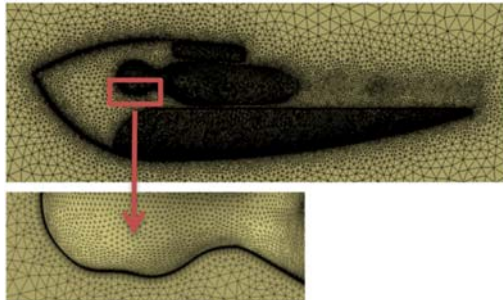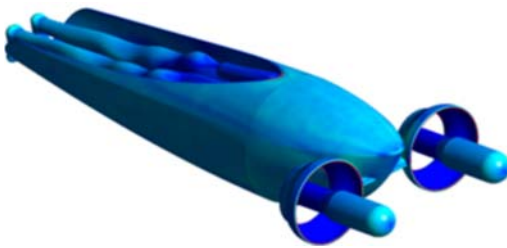

Fig. 4. Mesh generation with boundary layer elements in symmetric plane.

Fig. 5. The Y$^+$ distribution on DPV model in 6 m/s.

The second parameter that it is important to solution accuracy is velocity value in lateral boundaries relative to inlet velocity that must be has a negligible change with another. The satisfaction of this condition has been shown in Fig.6 by showing velocity distribution on boundary domain zone. When the deviation of velocity related to vehicle velocity in this boundary is less enough it will be attained that a good selection of domain size has been occurred. This margin is less than 0.17% in overall boundary surface that is acceptable for solution accuracy.
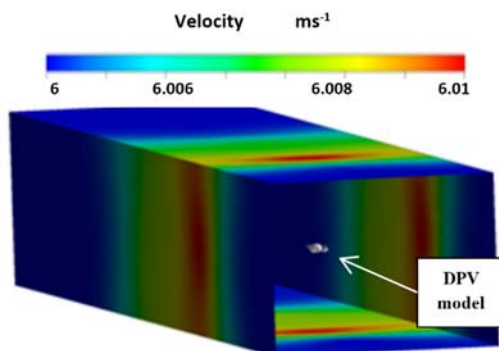

Fig. 6. The distribution of velocity on domain border.

The boundary conditions adopted for the CFD calculation are:

- Uniform known velocity in domain inlet

- Mass conservation law at exit

- The no-slip condition is imposed on the surface of the vehicle and diver body

- The condition of symmetry is imposed on the symmetric surface of the vehicle

Although the flow field is not perfectly symmetric because of shedding vortex behind it, for reducing the CPU time some simplification should be assumed. This simplification does not distort the solution procedure and only has a little variation on the final hydrodynamic coefficients that could be amended in final geometry.

In summary:

- The geometric model is produced,

- The solution domain is arranged,

- The grid is generated,

- The CFD analysis is completed and obtained hydrodynamic forces.

Then the results should be compared as checking optimization limitation step. Two objective functions were being made for optimization criterion in each iterative process to receive optimal shape as the main goals:

a) Hydrodynamic lift force ≈ 0 $(0 \leq L \leq 50\ N$)

b) $\delta D_i \approx 0$ (Minimum hydrodynamic drag Force)

$$(11)$$

The vehicle is designed as neutral buoyancy so hydrodynamic lift force is selected to zero. In fact it has been set as lift force less than 50N in calculating process as one of the stopping criteria. The curvature of upper and lower body surface is important to lift force value. In general the lift force tends to increase when the upper surface convexity will be increased and vice versa. As well as the lift force tends to decrease (or negative) when the lower surface convexity will be increased and vice versa. These phenomena are the basic concept of hydro-aerodynamic moving body that has been exerted as a mathematical modeling in the scenario. This process will be continued to satisfy the criterions.

Furthermore the drag force also must be minimized. It has been formulated in the code as the other stopping criteria:

$$\left| \frac{D_i - D_{i+1}}{D_i} \right| \leq 2.5\% \qquad (12)$$

Moreover another parameter that has been checked as secondary objective function is pitching moment that trace during each solution step out of code. It should be maintained relatively minimum also. The design parameters should be defined exactly and precisely until CPU time is accurately decreased, otherwise this process is prolonged and not worthwhile. Actually, each optimization loop will be

prolonged about 3.2 days (74-78 hours) and about 20 iterations are estimated for the whole process. A checking stop point has been put in each loop as when the GUI outputs are acceptable the process will be continued by designer supervisor. The GUI is a graphic user interface that should be linked to journal file of fluent code by MATLAB compiler editor. For linking geometry implementation software to solver software by enable re-meshing (Fluent) two links have been established by it, one to CATIA and the other to fluent. So each of basic control points in CATIA have been taken in the form of text file output format. Then the required conditions have been applied in it, i.e. the equations (9) and (10). In fact, realizing optimization parameters and interning by MATLAB code then converting this text file format to ANSYS Meshing input file, the geometry has been prepared to mesh generation. This high performance software produces the appropriate mesh for solution. Finally, the outputs of fluent are compared with constraints in MATLAB.

There are many design variables may be changed in optimization process but the most important one are the nose and body contour and propulsion unit level and its' longitudinal position that each one would be changed to satisfy intimated constraints in sequential algorithm. In each step the different trial nose shapes as Fig. 7 have been examined on the body and their results have been compared.

Really in each region of the body that high pressure difference has been occurred, focused on it and tried to reduce it by changing curvature of that region to receive the most uniform pressure distribution to approach the goal functions.
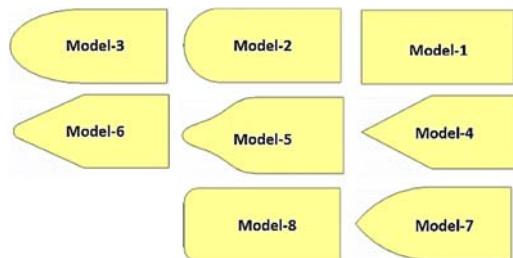

Fig. 7. Different nose that composed to the body in each iteration process.

Clearly when the constraint of Eq. (12) will not be satisfied the form of trailing body cone has been changed at first and the nose secondly. The convex angle of the aft body configuration that has been formed as frustum shape is one of design variables in the problem. As you know the water shield or diver's parapet will be produced high pressure region in nose and any aft body vertical partitions will be generated low pressure regions as suction side in the aft that both of them will be produced more drag. The interconnection of four main surface i.e. DPV upper and lower surface with left side and right side surface has been created minimum aft body vertical partition that has been considered in Geometry Implementation section. The pressure and velocity distribution are presented in Fig. 8 and Fig. 9 for final shape.
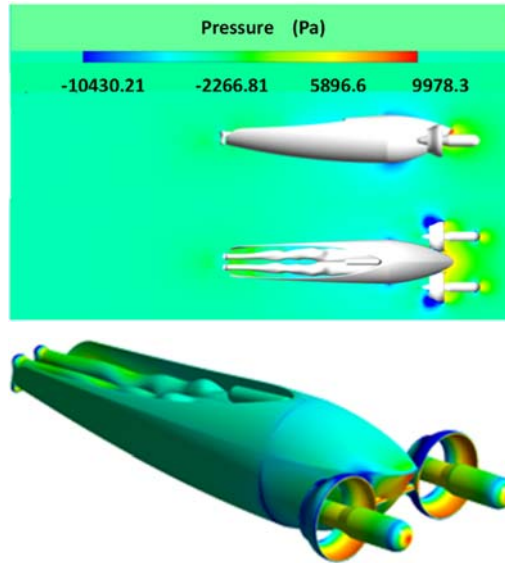

Fig. 8. Relative pressure distribution on vehicle, V=6 m/s.
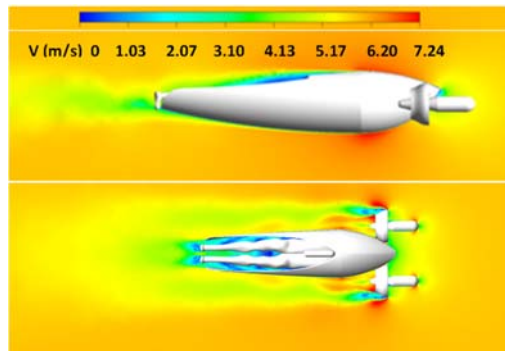

Fig. 9. Velocity distribution around the vehicle, V=6 m/s.

The maximum pressure region occurred at the motor leading edge and interior of the court nozzle. Based on foregoing the shape of vehicle has been gradually changed to last one in accordance to optimization loop.

4. CONDITIONS AND FACILITIES OF TOWING TANK LAB

The test conditions might be varied considerably depending on water density whereas the temperatures fluctuated from around 4°C to 30°C. Consequently, the fluid properties also will be varied considerably. Thus for the purposes of assimilating to international tests it is clearly convenient to adopt some reference conditions in accordance with *ITTC 2006 Recommended Procedures and Guidelines*. These rules are based on fresh water in 20.9°C with a density value of 1024.364 kg/m³. The kinematic viscosity υ in this temperature is 9.822e-7 m²/s. In experimental tests the towing speed should be varied considerably for obtaining favorable results. In test the model should be fixed in its position and applied identical conditions for each towing speed test. The experiments have been conducted in the pool with
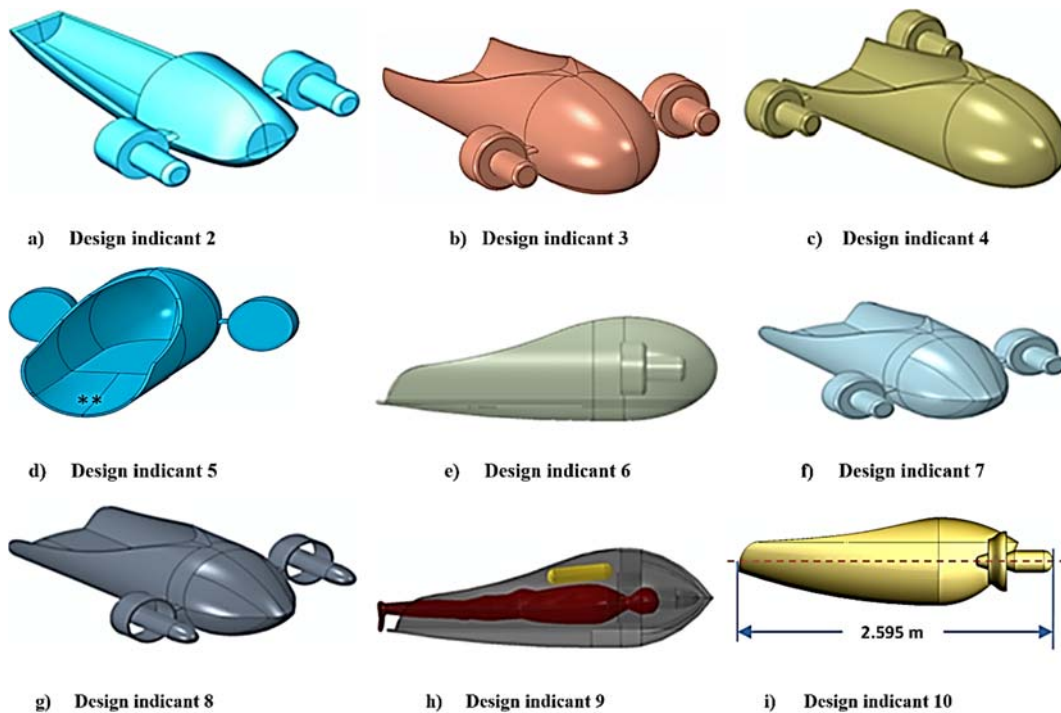
Fig. 10. Improvement of DPV configuration in optimization process at each design stage.

140 m length, 3.5 m depth and 7 m width and the towing force has been generated by using a 45 kilowatt electrical motor with inverter controller. In each case the temperature and density of water have been measured. The lab instruments supported each experiment by an industrial high speed computer and the test data like drag force, lift force, pitching moment, acceleration and speed have been recorded. All data were acquired by using a PC based National Instrument data acquisition system that has been sampled at 100Hz rate. The output data have been averaged in order to eliminating the effects of any unsteadiness and unfavorable noise and the averaged values have been stored for further analysis and comparison with numerical outputs. One underwater and two overwater cameras have been used for capturing the situations of the model during each experiment.

The dimensions of towing tank are large enough to avoid flow blockage effects. Namely, the tank cross section compared to model cross section is large enough whereas it has been satisfied the *ITTC 2002 rules*. The model frontal area is approximately between 0.39 to 0.41 m^2 and the pool cross sectional area is 22.5 m^2, so the blockage ratio is suitable for experimental tests.

5. RESULTS AND DISCUSSIONS

In summary, the difference between designs and their results of each indicant have been explained as follow with respect to (Fig. 10):

First Design: It is designed as a primary concept for starting designing scenario. That is based on real

prototype that had been presented for production. It was like K-10 TNT Marine Enterprises diver training propulsion vehicle sample. The preliminary dimensions of the first DPV had been selected as 2m×0.7m×0.7m (length ×width× height) based on a diver with 1.8 m height.

Design indicant 2 (Fig. 10a): The propulsion system is brought to fore and improvement on hydrodynamic forces occurred; indeed the drag force was reduced, (Fig. 11). Really this is unlike of anyone prediction and this will be rechecked again in next step. It may be because of pressure distribution pattern that causes reduce low pressure region in aft body.
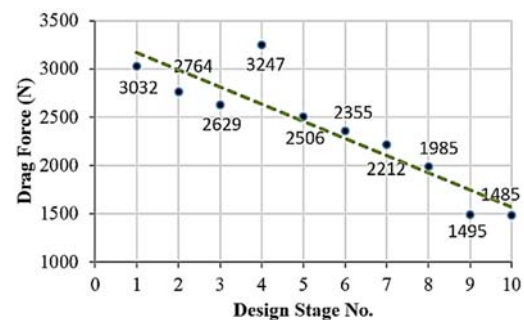

Fig. 11. The trend of drag force vs. each design.

The dash line shows the complete fall in the trend of results.

Design indicant 3 (Fig. 10b): The nose geometry is rounded and profile of upper and lower surface would be better for avoiding flow separation with respect to design indicant 2 and further decrease in drag force

was observed, (Fig.11). In this geometry the area of vertical plain has been deleted and high pressure region limited to very small area that tending to a point.

Design indicant 4 (Fig. 10c): The propulsion unit moved from fore to aft without any other change in shape. By comparing hydrodynamic forces to previous step, it would be proved that the best position of propulsion system is at the fore of the vehicle and in the same level of vehicle center of pressure. In fact, the drag and lift both increase when the propulsion is moved to aft position, Fig.11 and Fig. 12. Of course the frontal area was increased 2.56% in this step also but it seems that the propulsion relocation is further effect.
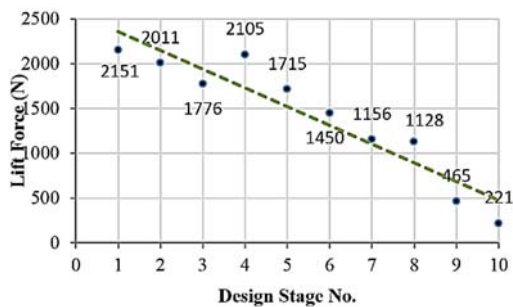

Fig. 12. The trend of lift force vs. each design.

Design indicant 5 (Fig. 10d): It is similar to design indicant 3 and the propulsion unit back to fore again and the bottom surface in aft region (**) is swept down to reducing aft vertical area because high pressure suction occurred in this region and it has been reduced by this aft reconfiguration. In this design stage the solution focused on aft of the vehicle geometry where suction has been increased. With this change, reducing trend of drag and lift forces have been observed again, Fig.11 and Fig. 12.

Design indicant 6 (Fig. 10e) : It is similar to previous design but an attempt to sweep down region would be transferred to outer surface and by removing the sharp edge in frontal flow side by rounding profile the other new geometry was produced.

Design indicant 7 (Fig. 10f): The nose region differs from previous step and better result has been attained. This form of nose has good characteristic according to the other later experience on dolphin and blue shark nose. With this nose modification a slight decrease in drag and more decrease in lift force were observed, Fig.11 and Fig. 12. In the blue shark nose the leading edge of nose sharper than dolphin and is attained more speed. In fact in this step the vertical area against flow stream has been minimized.

Design indicant 8 (Fig. 10g): In this stage the stagnation point of nose moved down about 5 cm with respect to later model by changing nose form and brought better pressure distribution in this region and reduced nose up pitching moment. Because the arm of force center of gravity was

decreased. A round spinner shape was used to propel inlet to improve intake flow stream. Also, the model of propulsion system has been improved. Also, the propeller modeling has improved for 800 rpm rotational speed to achieve better accuracy. But despite of drag force decreased the lift force increased Fig.11 and Fig. 12.

Design indicant 9 (Fig. 10h): The diver with standard air tank was considered because the convergence in solution was observed as well as and complete simulation accessible. The air tank has been caused to reduce back pressure suction region in upper surface. Meanwhile the lift force also should be decreased as possible. In fact, the separation in upper surface will be caused to accelerating the flow and generating higher lift force. This effect must be reduced whatever possible too, Fig.11 and Fig. 12.

Design indicant 10 (Fig. 10i): In the recent stage almost the final solution obtained but partial optimization has been taking placed. Namely the curvature of lower surface has been increased and the area of open surface in top of vehicle decreased. The more convexity of lower surface was caused to reduce pressure in this region and will be decreased lift in succeeding.

Based on the above explanation the trend of design is credible and this configuration could satisfy underwater diver motion. In the last stage the vertical position of propulsion system has been set on the center of pressure in vertical axis to avoid excess pitching moment at various propeller speed and according to the latest information from thruster producer, the geometry of court nozzle has been sized on it. In each step, the pressure and velocity distribution on vehicle were investigated and the shapes has been changed according to them.

The drag force measured from CFD is showed predictable trends Fig. 11 from modification of each design stage. Though this trend had a decreasing format, a maximum occurred in design stage 4. This behavior would be under control by author to show the accuracy of position of thruster system in iteration process. In so far as the drag might be minimized but the lift force might not be in the same manner. For this reason both limitations "a" and "b" of relation 11 should be satisfied. Along the drag curve the lift force curve has been showed a fluctuation but finally it will approach a suitable value. The final results of the research are comprise 51% decrease in drag (that will be trepanned to decreasing 51% of required power) and more than 89.7% decreasing in lift force. Of course this decreasing trend has been occurred for pitching moment that redounded to ease control and stability.

After attaining to final shape and the computation steps were completed, now the time of validation of numerical outputs is coming by towing tank experiments. Two models have been constructed and tested, one half scale and the other full scale. The images of model during the test have been shown in fig. 13.
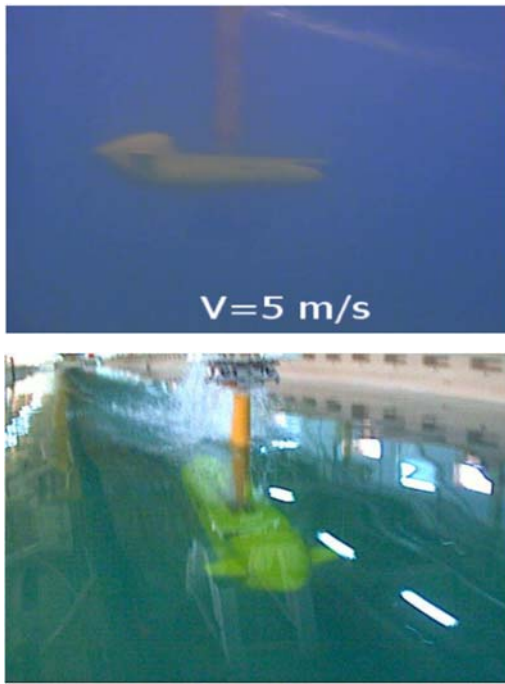
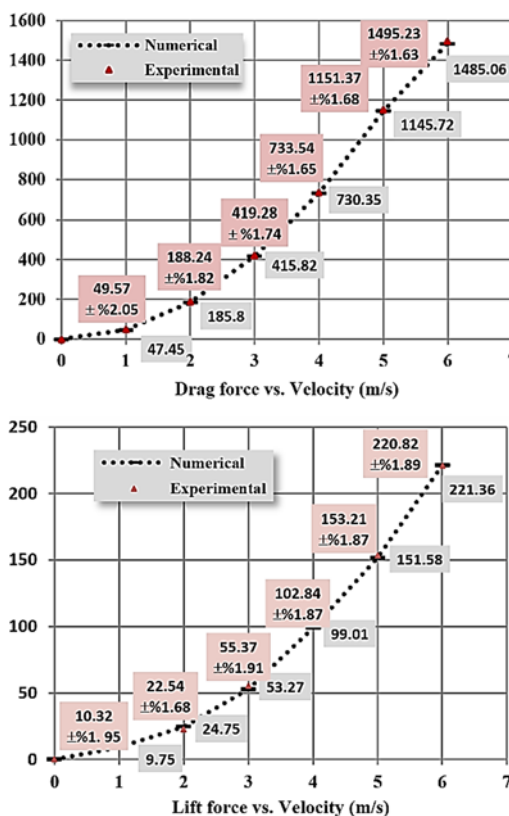**Fig. 13. The towing tank experiments, speed 5m/s.**

Fig. 14. The comparison of numerical and towing tank experimental output.

The experiment has been done for 6 speeds and in 1.5m depth and the hydrodynamic forces have been registered. The drag–velocity curves exhibit a smooth second order behavior that approaches to maximum 1645.57N in 6 m/s, Fig. 14. In the

maximum speed the power required to overcome to resistive force is about 10.125Kw according to Eq. (7). If an electrical propulsion system is going to be used with propulsion efficiency of 75% (for propeller and electrical motor) the power capacity that should be installed is equal to 13.5Kw. It is very important to reach this performance under water and obtain a new recording speed which is not antecedent heretofore. Of course for extracting the forces in other speed numerically we used CFD loop of optimization process alone and it is considered that the numerical computation has accurately accordance to test results. The maximum deviations between experimental and numerical results of drag force are 4.3% and 5% for lift force that is really acceptable. The error analysis that was derived from test results standard deviation has been calculated by LAB-VIEW software automatically for four repeats in each test which show maximum 4.2% deviation values in each of the relevant data.

6. CONCLUSIONS

This paper has been demonstrated an optimization scenario to modifying an arbitrary DPV for diver motion up to 6 m/s velocity that there is not antecedent heretofore. By presented optimization method each designer are going to be able to optimizing underwater vehicle by 3D CFD method where important issues such as diver ergonomic, drag and lift force limitations or other limitation have been considered. The arrangement of objective functions are very easy and may be entered other required goal function to the code. Also, the simple restriction has been considered into problem. Though this process will be required a long time computing with hydrodynamic design skills that could be controlled the process as a skillful supervisor. Especially in model implementation module you should be cooperated with machine to response to the checking question truly.

Of course, other hydrodynamic characteristics such as pitching moment might be considered too. This parameter could be entered in goal function but will be caused paper voluminous but it is very important nonetheless in real applicable products dynamic and stability motion.

You must be remind that with entering each goal function the solution will be more prolonged but in this paper has been presented a simple applicable model for solving problem like this. As you mentioned there are many required parameter that you will be needed in output results.

REFERENCES

Bixler, B. S. and M.Schloder (1996). Computational fluid dynamics: an analytical tool for the 21st century swimming scientist. Journal of Swimming Research 11, 4–22.

COHEN, R. C. Z. and *et al.* (2009). Simulations of Human Swimming Using Smoothed Particle Hydrodynamics, Seventh International Conference on CFD in the Minerals and Process Industries, CSIRO, Melbourne, Australia.

Frederic, P. *et al.* (2010). Diver Propulsion Vehicle book, by VDM Publishing, ISBN 6130783159, 9786130783150.

Griffiths, G. and I. Edwards (2003). Designing and operating next generation vehicles, Elsevier Oceanography Series 69, 229–236.

Ishak, D. and *et al.* (2010). Electrically Actuated Thrusters for Autonomous Underwater Vehicle, The 11th IEEE International Workshop on Advanced Motion Control, Nagaoka, Japan.

ITTC Recommended Procedures and Guidelines (2002). Testing and Extrapolation Methods for Resistance Test, 7.5-02-02-01 and Blockage Corrections 3.6.3, 8.

ITTC Recommended Procedures and Guidelines (2006). Edited by 22nd ITTC QS Group for Testing and Extrapolation Methods, 7.5-02-01-03 and General Density and Viscosity of Water, Values of Mass Density for Salt Water, page 4 table 2.

Ramos, R. and *et al.* (2012). The Effect of Body Positions on Drag During The Streamlined Glide: A Three-Dimensional CFD Analysis, Journal of Biomechanics.

Sadeghizadeh, M. R. and *et al.* (2016). Experimental and Numerical Investigation of High Speed Swimmer Motion Drag Force in Different Depths from Free Surface, *Journal of Applied Fluid Mechanics* 10(1).

Smallwood, D. and *et al.* (1999). A new remotely operated underwater vehicle for dynamics and control research," in Proceedings UUST '99.

Tahara, Y. and *et al.* (2006). CFD-based multi-objective optimization method for ship design, International Journal for Numerical Methods in Fluids.

Zaidi, H. and *et al.* (2010). Turbulence model choice for the calculation of drag forces when using the CFD method, Journal of Biomechanics 43(2010)405–411.